

Nonresonant holeburning in the Terahertz range: Brownian oscillator model

Uli H aberle and G regor D iezem ann

Institut für Physikalische Chemie, Universität Mainz, W elderweg 11, 55099 M ainz, FRG

The response to the field sequence of nonresonant holeburning, a pump-probe experiment originally designed to investigate slow relaxation in complex systems, is calculated for a model of Brownian oscillators, thus including inertial effects. In the overdamped regime the model predictions are very similar to those of the purely dissipative stochastic models investigated earlier, including the possibility to discriminate between dynamic homogeneous and heterogeneous relaxation. The case of underdamped oscillations is of particular interest when low-frequency excitations in glassy systems are considered. We show that also in this situation a frequency selective modification of the response should be feasible. This means that it is possible to specifically address various parts of the spectrum. An experimental realization of nonresonant holeburning in the Terahertz regime therefore is expected to shed further light on the nature of the vibrations around the so-called boson peak.

PACS Numbers: 64.70 Pf, 05.40.+j, 61.20.Lc

I. Introduction

The relaxation functions observed in disordered materials such as glasses, spin-glasses, disordered crystals or proteins are usually found to decay non-exponentially on macroscopic time scales [1]. Several experimental techniques have been invented in order to investigate the detailed nature of this non-exponentiality, among them a reduced four-dimensional NMR technique [2], an optical deep bleach experiment [3] and also nonresonant holeburning (NHB) [4]. Common to all the techniques is that they allow to specifically select a (slow) sub-ensemble and afterwards monitor its relaxation. This way the existence of dynamic heterogeneities could be verified experimentally [5]. In the present paper we adopt the definition given in ref. [6] according to which a response or relaxation function is termed dynamic heterogeneous if it is possible to specifically address effectively slow, intermediate or fast contributions to the ensemble averaged function. Otherwise, the relaxation will be termed dynamic homogeneous. It is important to mention that neither this definition nor any of the quoted experiments allow to obtain information about any spatial aspects of these heterogeneities.

NHB consists of a pump-wait-probe field sequence, starting with the application of one (or more) cycles of a large amplitude ac field with frequency ω to the sample in equilibrium. After a waiting time t_w has elapsed, a small field is turned on to monitor the modified response, cf. Fig. 1. A qualitative interpretation of the experimental results relies on the fact that via the application of the ac field the sample absorbs energy of an amount proportional to the imaginary part of the susceptibility evaluated at the pump-frequency [7]. One thus expects that a frequency selective modification of the spectrum should be feasible only if the response is given by a heterogeneous superposition of entities relaxing at different rates. This view has proven fruitful in the interpretation of experimental results obtained from a variety of samples, including supercooled liquids [4, 8], disordered crystals [9], amorphous ion-conductors [10] and spin glasses [11]. A theoretical investigation in terms of a response theory has been developed for the case of stochastic dipole-reorientations [12], which has shown that the modified response indeed depends on the absorbed energy, thus supporting the above picture [13].

At this point a note of caution is appropriate. NHB differs fundamentally from the so-called spectral holeburning experiment known from nonlinear optics [14], which e.g. has successfully been used to investigate the dynamics of two-level systems in glasses [15]. In this experiment the optical transition of a dye molecule is altered externally, thus giving rise to a hole in the remaining absorption spectrum. In contrast, NHB does not work at frequencies allowing to monitor electronic transitions and we are concerned with dynamic features which are much slower.

Because the mentioned theoretical investigation on NHB [12] was concerned with slow reorientational dynamics, typically on a time scale of μ s, only purely dissipative dynamics has been considered and inertial effects have been neglected completely. Given the fact that the primary relaxation of supercooled liquids is of a dynamic heterogeneous nature, the question as to which extent the same holds for the fast dynamics in these systems naturally arises. In particular, this point may prove of importance for understanding the physical origin of the so-called boson peak, observable e.g. as low-frequency oscillations in nonresonant Raman scattering [16]. On the experimental side, the recent developments in far-infrared spectroscopy [17], in particular the application of femtosecond Terahertz pulses [18] have opened the way to investigate the nonlinear dielectric response in this frequency range in detail. Thus, there is good reason to hope that the realization of an experimental protocol like the NHB field sequence should not be out of reach in due course [19].

In this paper we present a theoretical analysis of NHB for the case of damped oscillations using the well known model of Brownian oscillators (BO) [14]. This model, which often is employed in calculations of the nonlinear optical response in condensed phases, allows us to treat both, underdamped and overdamped motions in a coherent way. The outline of the paper is as follows. In the next section we describe the model and the theoretical aspects of our study. Section III contains the results of the model calculations along with

the discussion, including an estimate of the expected magnitude of the nonlinear effects. Finally, we close with some concluding remarks in Sect. IV.

II. NHB for the Brownian Oscillator Model

In this section we briefly discuss those features of the BO model that will be relevant for our discussion. Additionally, we calculate the linear and the third-order response functions relevant for the NHB experiment. As we are primarily concerned with the response of amorphous systems, we have to face the problem of treating spatial correlations of the coefficients in a normal mode expansion of the dipole moments. Therefore a discussion of the frequency dependence of the so-called light to vibration coupling constant is included.

A. General aspects and linear response

We assume that the normal modes $f_{qj} = f_{qj}; q_j$ of the system under consideration in the THz regime can be approximated as independent oscillators. In a molecular system, the q_j would correspond to internal degrees of freedom like vibrational or torsional modes and in a macroscopic system like an amorphous system the q_j represent all vibrational excitations including the low-frequency phonon-like collective modes.

In the classical version of the BO model with Markovian damping (Ohmic friction) [14] and equal masses, $m_j = m$, the dynamics of the q_j is described by the Langevin equation:

$$m \ddot{q}_j + m \gamma_j \dot{q}_j + \frac{dV(f_{qj})}{dq_j} = \xi_j(t) - \frac{\partial H_{int}}{\partial q_j} \quad (1)$$

Here, γ_j denotes the damping constant and $\xi_j(t)$ is a Gaussian stochastic force with zero mean and correlation $\langle \xi_j(t) \xi_k(t') \rangle = 2 \gamma_j k_B T \delta_{jk} \delta(t - t')$, k_B is the Boltzmann constant. Furthermore, the coupling to the field, H_{int} , is given by [14]:

$$H_{int} = \sum_j \int dr (r; f_{qj}) E(r; t) \quad (2)$$

The Fokker-Planck equation corresponding to the Langevin equation, eq.(1), is solved using the harmonic case as the unperturbed model and treating anharmonic terms in $V(f_{qj})$ as well as H_{int} in perturbation theory similar to the calculation performed in ref.[12]. We mention that the assumption of Ohmic friction can easily be relaxed and a dynamic homogeneous scenario can be modelled via a frequency dependent damping ($\gamma(\omega)$). This case, however, is most relevant for overdamped motions and will be treated in a forthcoming publication [20]. The solution of eq.(1) shows that all quantities of physical interest are determined by $\gamma_{j1} = \frac{1}{2}(\gamma_j + \gamma_j)$ and $\gamma_{j2} = \frac{1}{2}(\gamma_j - \gamma_j)$ with $\gamma_j = (\frac{2}{\gamma_j} - 4\gamma_j^2)^{1/2}$.

In order to calculate the response to an external electric field, we expand the dipole moment

$$\begin{aligned} \langle r; f_{\text{qg}} \rangle &= \langle r \rangle_0 + \sum_i \langle r \rangle_i^0 q_i + \frac{1}{2} \sum_i \langle r \rangle_i^{00} q_i^2 + \dots \\ \text{with } \langle r \rangle_i^0 &= \frac{\partial \langle r \rangle}{\partial q_i} \Big|_0 \quad \text{and} \quad \langle r \rangle_i^{00} = \frac{\partial^2 \langle r \rangle}{\partial q_i^2} \Big|_0 \end{aligned} \quad (3)$$

and neglect higher order terms as well as cross-terms for simplicity. We will focus on the dielectric response but the inclusion of a similar expansion of the polarizability, relevant for Raman scattering, poses no problem. Note that we have kept the position-dependence of the dipole moment, since in amorphous systems correlations are expected to exist which extend over some finite volume, depending on the coherence length of the modes q_i [21].

In the present model, there are different contributions to a non-vanishing third-order response [22]. One nonlinear term stems from the quadratic term in eq.(3). Another possible source of nonlinearity has its origin in anharmonic contributions to the potential. In our calculations, we use a potential of the form $V(f_{\text{qg}}) = \sum_i V(q_i)$ with

$$V(q_i) = m_i \frac{1}{2} \omega_i^2 q_i^2 + \frac{1}{3} \gamma_3 q_i^3 + \frac{1}{4} \gamma_4 q_i^4 + O(q_i^5) \quad (4)$$

where we have scaled the anharmonicity strengths by the harmonic frequency ω_i^2 . Higher-order terms in the potential and also a coupling among the q_i can easily be incorporated albeit this leads to an increasing number of parameters.

The polarization following the NHB field sequence for a single mode q_i is calculated in $O(E_P^2)$ and $O(E_M)$. Without going into the details of the calculations here, we mention that the NHB-response $P_i^{(X)}(t; t_w; t_p)$ is given as a superposition of the ordinary linear response and a modification:

$$P_i^{(X)}(t; t_w; t_p) = P_i^{(X)}(t) + P_i^{(X)}(t; t_w; t_p) \quad (5)$$

Here, $P_i^{(X)}(t)$ denotes the polarization in $O(E_M)$. In addition, the nonlinear modification, $P_i^{(X)}(t; t_w; t_p)$, which is $O(E_P^2)$, contains various terms, to be discussed later. Note that the form of the signal is formally identical to the one found in ref.[12]. Thus the same phase-cycling as described in ref.[4] can be applied in order to extract the modification $P_i^{(X)}$. The superscripts 'X' stand for the different response functions measured. In the present paper we will discuss three different functions. A field pulse yields the pulse-response ($X=P$), while application of a constant field gives the step-response ($X=S$), also called the integrated response. Furthermore, we consider the response to an oscillatory field, denoted by $X=AC$. Summarizing, we have:

$$X=S : E_M(t) = E_M(t) \quad ; \quad X=P : E_M(t) = E_M(t) \quad ; \quad X=AC : E_M(t) = E_M e^{i\omega t}$$

where the fields in eq.(2) are given by $E(r; t) = e^{ik \cdot r} E(t)$.

Denoting the wave vector of the measuring field by k_M , one has for the polarization in the linear response regime:

$$P_i^{(X)}(t) = \frac{1}{m} E_M \int_{-Z}^Z dr_0 \int_{-Z}^Z dr_1 (r_0)_i^0 (r_1)_i^0 e^{ik_M r_1} R_i^{(X)}(t) \quad (6)$$

Here, $n = N/V$ is the number density of oscillators and $R_i^{(X)}(t)$ denotes the linear response of mode 'i'. The latter are different for different time-dependencies of $E_M(t)$.

In case of the pulse-response we have:

$$R_i^{(P)}(t) = \frac{1}{i} e^{-i\omega_2 t} - e^{-i\omega_1 t} \quad (7)$$

The integrated response function is trivially related to the pulse-response via $R_i^{(S)}(t) = \int_{-\infty}^t R_i^{(P)}(\tau) d\tau$ and the response to an ac field of frequency ω reads as:

$$R_i^{(AC)}(t) = \frac{1}{i} \frac{1}{i\omega_2} (e^{i\omega t} - e^{-i\omega_2 t}) - \frac{1}{i\omega_1} (e^{i\omega t} - e^{-i\omega_1 t}) \quad (8)$$

In the steady state, characterized by $e^{-i\omega_1 t} = 0$, this expression coincides with the Fourier transform of $R_i^{(P)}(t)$ according to eq.(7) up to the factor $e^{i\omega t}$. This is exactly the result expected from linear response theory [7].

B. Nonlinear modifications

There are various contributions to the cubic response and therefore also to the nonlinear modification of the response in a NHB field sequence. These stem from the higher order terms in the expansion of the dipole moment, eq.(3), and the anharmonic terms in the potential, eq.(4). In the lowest nonvanishing order, there are three relevant terms. One term has its origin in the quartic anharmonicity, χ_4 , along with the first order term in the expansion of the dipole moment. In the following, this term will be denoted as $P_i^{(X)}(t; t_w; t_p)$. In addition, there is one term, denoted by $P_{i,(\text{harm})}^{(X)}(t; t_w; t_p)$, which stems from the second order term in eq.(3) and the harmonic contribution to $V(\text{fpg})$. Finally, there exists one term which mixes the second order dipole moment term with the one of the cubic anharmonicity, which we will call $P_{i,(\text{mix})}^{(X)}(t; t_w; t_p)$. The principal features of these terms are very similar with quantitative differences only.

The different contributions are given by:

$$P_i^{(X)}(t; t_w; t_p) = \frac{3}{2m^3} \int_{-Z}^Z dr_0 \int_{-Z}^Z dr_1 \int_{-Z}^Z dr_2 \int_{-Z}^Z dr_3 (r_0)_i^0 (r_1)_i^0 e^{ik_M r_1} (r_2)_i^0 (r_3)_i^0 e^{ik_P (r_2 + r_3)} R_i^{(X)}(t; t_w; t_p) \quad (9)$$

Here, $R_i^{(X)}(t; t_w; t_p)$ denotes the intrinsic modification of mode 'i' and k_P and k_M are the wave vectors of the pump-field and the measuring field, respectively.

From eq.(9), the expression for $P_{i;(\text{harm})}^{(X)}(t; t_w; t_p)$ is obtained by dividing with $(\frac{3}{2} - 4)$, replacing $(r_k)_i^0, k=1;2$ by $(r_k)_i^0$ and using $R_{i;(\text{harm})}^{(X)}(t; t_w; t_p)$ instead of $R_i^{(X)}(t; t_w; t_p)$. In order to get the expression for $P_{i;(\text{mix})}^{(X)}(t; t_w; t_p)$ one has to multiply $P_i^{(X)}(t; t_w; t_p)$ in eq.(9) by an overall factor $(\frac{3}{2} - 4)$. Furthermore, $R_i^{(X)}(t; t_w; t_p)$ has to be replaced by $R_{i;(\text{mix})}^{(X)}(t; t_w; t_p)$ and one of the three $(r_k)_i^0, k \neq 0$, by $(r_k)_i^0$.

The expressions for the modification $R_i^{(X)}(t; t_w; t_p)$ (and also $R_{i;(\text{harm})}^{(X)}, R_{i;(\text{mix})}^{(X)}$) are somewhat more complex than those for the linear response. Here, we concentrate on $R_i^{(X)}$ and only mention that the other expressions are of a similar structure without giving them explicitly.

It turns out that for all three measuring procedures, $X = S, P$, and AC , the modification can be written in the form :

$$R_i^{(X)}(t; t_w; t_p) = \frac{1}{3} \frac{2!}{i} e^{2 - i;2 t_w} \hat{\Lambda}_{i;2}(\cdot) {}^2 h^X(i;1; i;2; t) e^{2 - i;1 t_w} \hat{\Lambda}_{i;1}(\cdot) {}^2 h^X(i;2; i;1; t) e^{(- i;1 + - i;2) t_w} \hat{\Lambda}_{i;1}(\cdot) \hat{\Lambda}_{i;2}(\cdot) g^X(i;1; i;2; t) \quad (10)$$

In this expression, the functions $\hat{\Lambda}_{i; }(\cdot)$ are defined by:

$$\hat{\Lambda}_{i; }(\cdot) = \frac{1}{\frac{2}{i} + 2} 1 - e^{-i; t_p} \quad ; \quad i = 1;2 \quad ; \quad t_p = \frac{2N}{\cdot} \quad (11)$$

with N denoting the number of cycles of the pump pulse. The functions $h^X(a;b;t)$ and $g^X(a;b;t)$ are linear combinations of exponential functions of time, given explicitly in the appendix. We mention that $R_i^{(P=S)}(t; t_w; t_p)$ are real quantities despite the fact that the $i; , i = 1;2$, are complex in the underdamped case.

From the expression for the modifications $R_i^{(X)}(t; t_w; t_p)$, eq.(10), it is evident that the absorbed energy plays an important role, albeit the situation is more complex than in case of a completely overdamped motion. It can be shown from eq.(10), using the expressions given in the appendix, that the modification vanishes in the limit of small as well as large times for $\gamma > 0$ and thus is of a transient nature. During the waiting time the created non-equilibrium population relaxes due to the term $e^{-i; t_w}$. This is because there is no extra relaxation mechanism in this model[12].

Eq.(11) shows that $\hat{\Lambda}_{i; }(\cdot) \rightarrow 0$ for $i; \rightarrow 0$ and $\hat{\Lambda}_{i; }(\cdot) \rightarrow 1$ for $i; \rightarrow 1$ and therefore the modification vanishes in these cases also. These considerations show that the nonlinear modification of the model considered in ref.[12] and of the BO model are very similar, particularly in the overdamped regime, which will be treated in more detail in the next Section.

Because we mainly are interested in oscillatory motions, we consider the signals in the frequency-domain as well. Here, the pulse-response is of particular importance as this is the quantity that is directly related to the complex dielectric constant in the linear regime. Therefore, in addition to the time-domain signals we will consider the Fourier

transformations of $R_i^{(P)}(t)$ and $R_i^{(P)}(t; t_w; t_p)$ with respect to the measuring time t . However, it is important to point out that the linear relation between the pulse-response and the step-response, $R_i^{(S)}(t) = \int_0^t R_i^{(P)}(\tau) d\tau$, does not hold for the modifications $R_i^{(S)}(t; t_w; t_p)$ and $R_i^{(P)}(t; t_w; t_p)$ due to the nonlinear nature of these functions. Similarly, there is no simple relation between the Fourier transform of $R_i^{(P)}(t; t_w; t_p)$, denoted as $R_i^{(P)}(\omega; t_w; t_p)$ in the following and $R_i^{(AC)}(\omega; t_w; t_p)$. This can be inferred from the definitions of the functions h^{AC} and g^{AC} , eq.(A.3). For long times the modification measured in the frequency domain, $R_i^{(AC)}(\omega; t_w; t_p)$, vanishes and there is no stationary state evolving as it is the case in the linear response, cf. eq.(8). This can be seen from eq.(A.3) as there is no term of the form $e^{i\omega t}$, but ω occurs solely in combinations with ω_i . Of course, this behavior also is to be expected intuitively because the modification is to be viewed as a transient effect. It is for this reason that we consider $R_i^{(P)}$ in the frequency domain.

C. Overdamped limit: Ornstein-Uhlenbeck process

As discussed above, the relation $dP^{(S)}(t)/dt = P^{(P)}(t)$ does not hold for the non-linear responses. This fact can be shown to hold true for non-linear response functions in general. Here, we will demonstrate it explicitly for the limiting case of a strongly overdamped motion, the so-called Ornstein-Uhlenbeck (OU)-process [23]. All expressions for the OU-process can be obtained from the corresponding ones for the BO-model from the lowest-order term of an expansion in $1/\gamma_i$. This expansion can either be performed on the Fokker-Planck equation itself or on any of the resulting expressions for the linear or nonlinear response. For the OU-process, the effective relaxation rate is given by $\gamma_i = \gamma_i^2/\gamma_i$ [14]. Additionally, the expressions for $R_i^{(S)}$ and $R_i^{(P)}$ obtained that way allow a direct comparison with those obtained for the model of stochastic dipole reorientations in ref.[12]. The linear response given in eq.(7) simplifies to

$$R_i^{(P)}(t)_{(OU)} = \frac{\gamma_i}{\gamma_i^2} e^{-\gamma_i t} \quad \text{and} \quad R_i^{(S)}(t)_{(OU)} = \frac{1}{\gamma_i^2} (1 - e^{-\gamma_i t})$$

For the modifications, however, one finds from eq.(10):

$$\begin{aligned} R_i^{(P)}(t; t_w; t_p)_{(OU)} &= \frac{\gamma_i}{\gamma_i^6} A_i(\omega) e^{-\gamma_i^2 t_w} (1 - e^{-\gamma_i^2 t}) e^{-\gamma_i t} \\ R_i^{(S)}(t; t_w; t_p)_{(OU)} &= \frac{1}{\gamma_i^6} A_i(\omega) e^{-\gamma_i^2 t_w} (1 - e^{-\gamma_i^2 t})^2 e^{-\gamma_i t} \end{aligned} \quad (12)$$

Here, the pump-frequency dependent amplitude is given by $A_i(\omega) = [\omega_i(\omega)]^2 (1 - e^{-\gamma_i t_p})^2$ with $\omega_i(\omega) = \gamma_i(\omega - \omega_i)$. It is evident from these expressions that $R_i^{(S)}(t; t_w; t_p) \notin \int_0^t R_i^{(P)}(\tau; t_w; t_p) d\tau$. Furthermore, the expression for $R_i^{(S)}(t; t_w; t_p)_{(OU)}$ is similar to the one found in ref.[12] for stochastic dipole reorientations apart from some minor differences, which will be discussed in detail elsewhere [20].

If we consider the Fourier transform of $R_i^{(P)}(t)_{(OU)}$, $R_i^{(P)}(!)_{(OU)} = !^2_i R_i^{(P)}(!)$ and compare it to the signal measured in the frequency domain via application of a field $E_M e^{i!t}$,

$$R_i^{(AC)}(t)_{(OU)} = !^2_i R_i^{(P)}(!) e^{i!t} e^{-i!t};$$

for $t \rightarrow 0$ one finds the standard result of linear response theory, namely $R_i^{(AC)}(t)_{(OU)} = e^{i!t} R_i^{(P)}(!)_{(OU)}$. However, this does not hold for the modification $R_i^{(AC)}(t; t_w; t_p)_{(OU)}$. According to eq.(10), we have:

$$R_i^{(AC)}(t; t_w; t_p)_{(OU)}^0 = \frac{1}{!^6_i} A_i(!) e^{-2 i t_w} !^2_i (!) \left[2 i e^{-2 i t} \frac{\sin(!t)}{!} + (e^{3 i t} - e^{-i t}) \right]$$

which has to be compared to the imaginary part of

$$R_i^{(P)}(!; t_w; t_p)_{(OU)} = \frac{1}{3!^6_i} A_i(!) e^{-2 i t_w} [\beta_i(!) - \beta_i(!=3)] \quad (13)$$

Whereas the dependence on the burn frequency is identical, this does obviously not hold with respect to the frequency $!$. The modification $R_i^{(AC)}(t; t_w; t_p)_{(OU)}^0$ clearly exhibits a transient behavior with respect to the time t as it vanishes in the limit of short and long times. There is no stationary state which would allow to set a time-window for observation, in marked contrast to the linear response. These considerations show that it is most meaningful to consider $R_i^{(P)}(!; t_w; t_p)$, i.e. the Fourier transform of $R_i^{(P)}(t; t_w; t_p)$, in the frequency domain and not the signal measured via application of an ac-field.

D. Light to vibration coupling

As already noted above, in amorphous systems spatial correlations of the dipole moments are expected to exist which extend over some finite volume, depending on the coherence length of the modes q_i . Therefore, the position-dependence of the $\langle r_i^0 \rangle$ and the $\langle r_i^0 \rangle_i$ plays an important role. This fact complicates the relation between the intrinsic response functions and the respective polarizations, eqns.(6) and (9). Thus, the situation is very similar to the case of Raman scattering in glasses[21].

In the expression for the linear response, eq.(6), we have to consider the correlation function $\int dr_0 \int dr_1 \langle r_0 \rangle_i^0 \langle r_1 \rangle_i^0$, where we have used $e^{ik_M r_1} \approx 1$, i.e. the $k \rightarrow 0$ limit of $\hbar \langle k \rangle_i^0 \langle k \rangle_i^0$. In order to proceed in the calculation of this function, we make the same assumptions as they are typically used in calculations of the Raman-scattering intensity from amorphous systems[21, 24]. We assume that the coherence length of the mode q_i is much smaller than the wavelength of the light. Additionally, we disregard the dependence of all quantities on the polarization of the mode q_i and of the light. In an amorphous system $\hbar \langle k \rangle_i^0 \langle k \rangle_i^0$ is expected to have a broad maximum in the vicinity of $k = 0$, in vast contrast to the situation in crystals. This is the reason for the breaking of the momentum

transfer selection rules in the case of Raman-scattering [21]. A comparison of our expression to the ones obtained for the Raman-scattering intensity shows that $h(\mathbf{k}_\lambda^0(\mathbf{k})_i^0)$ is proportional to the so-called light to vibration coupling $C(!_i)$. Indeed, a very similar behavior of the Raman- and Infrared-coupling constants has been observed in a silica glass [25]. We thus assume $h(\mathbf{k}_\lambda^0(\mathbf{k})_i^0) = C(!_i)$ apart from an overall prefactor $j_i^{0,2}$, which replaces $j_i^{0,2}$ occurring in the Raman case, i.e.

$$h(\mathbf{k}_\lambda^0(\mathbf{k})_i^0) = j_i^{0,2} C(!_i) \quad (14)$$

In the expression for the modification $P_i^{(\chi)}$, eq.(9), the four-point correlation function $h(r_0)_i^0(r_1)_i^0(r_2)_i^0(r_3)_i^0$ occurs. In general such quantities are extremely difficult to calculate. Therefore, in order to be able to proceed we assume that the probability generating functional for the correlations can be represented by a Gaussian. Note that this is exact for harmonic vibrations and otherwise represents a mean-field approximation for the spatial correlations of the modes q_i . With this approximation the four-point correlations factor into products of two-point correlations yielding

$$\int dr_0 \int dr_1 \int dr_2 \int dr_3 (r_0)_i^0 (r_1)_i^0 (r_2)_i^0 (r_3)_i^0 e^{i[\mathbf{k}_M \cdot \mathbf{r}_1 + \mathbf{k}_P \cdot (\mathbf{r}_2 + \mathbf{r}_3)]} = 3 j_i^{0,4} C(!_i)^2$$

in the expression for $P_i^{(\chi)}$, eq.(9).

For $P_{i;(harm)}$ another four-point correlation function, $h(r_0)_i^0(r_1)_i^0(r_2)_i^0(r_3)_i^0$ occurs, cf. the discussion in the context of eq.(9). In the mean-field approximation one thus has to deal not only with $h(\mathbf{k}_\lambda^0(\mathbf{k})_i^0)$, but also with the unknown correlation functions $h(\mathbf{k}_\lambda^0(\mathbf{k})_i^0)$ and $h(\mathbf{k}_\lambda^0(\mathbf{k})_i^0)$. For the function $h(\mathbf{k}_\lambda^0(\mathbf{k})_i^0)$ it is reasonable to assume that it is vanishingly small in isotropic systems because of the odd number of derivatives. We thus assume

$$h(\mathbf{k}_\lambda^0(\mathbf{k})_i^0) = 0 \quad (15)$$

For the function $h(\mathbf{k}_\lambda^0(\mathbf{k})_i^0)$ one expects a similar behavior as for $h(\mathbf{k}_\lambda^0(\mathbf{k})_i^0)$. In general, however, the frequency-dependences may be different. Therefore, we write

$$h(\mathbf{k}_\lambda^0(\mathbf{k})_i^0) = j_i^{0,2} C^0(!_i) \quad (16)$$

and this way find

$$h(r_0)_i^0(r_1)_i^0(r_2)_i^0(r_3)_i^0 = j_i^{0,2} j_i^{0,2} C(!_i) C^0(!_i)$$

Only if one assumes in an ad hoc manner that the $(r)_i^0$ couple to the same elasto-optical constants as the $(r)_i^0$ one has $C^0(!_i) = C(!_i)$ in the expression for $P_{i;(harm)}$. Due to the lack of a theoretical argument in favor of such an approximation we mainly focus on $P_i^{(\chi)}$ throughout the present paper.

The last term occurring in eq.(9) is the 'cross-term' $P_{i;(mix)}^{(\chi)}$. The relevant four-point correlation function in this context is $h(r_0)_i^0(r_1)_i^0(r_2)_i^0(r_3)_i^0$. However, in every term

of the mean-field approximation the two-point correlation function $h(k)_i^0(k)_i^0$ occurs. Therefore, due to eq.(15) we approximately have

$$P_{i;(m \rightarrow x)}^{(\alpha)}(t; t_w; t_p) \neq 0$$

Various models for the low-frequency excitations in glasses have been used to calculate $C(\omega_i)$. All of them yield power laws, $C(\omega_i) \propto \omega_i^n$, with exponents n ranging from $n=0$ in the soft potential model [26] to $n=2$ in the harmonic model [24]. Furthermore, when $C(\omega_i)$ is analyzed via a comparison between experimental Raman- and neutron-scattering intensities from the same sample [27] often a $C(\omega_i) \propto \omega_i$ dependence is found. Also a nonvanishing limiting value $C(\omega_i \rightarrow 0) \neq 0$ has been reported [28]. It also should be mentioned that even an explicit k -dependence of the low-frequency Raman-scattering intensity has been observed in a silica glass [29]. Thus, given the uncertainty regarding the light to vibration coupling, in the present paper we will use $C(\omega_i) \propto \omega_i^n$ with $n = 0; 1; 2$ in order to discuss the possible behavior.

In actual calculations, we furthermore disregard the dependence of $\langle r \rangle_i^0$ on the mode-index i and write for the coupling constant

$$h(k)_i^0(k)_i^0 = j_{ij}^0 j_{ij}^0 C(\omega_i) \quad \text{with} \quad C(\omega_i) \propto \omega_i^n \quad (17)$$

It should be noted that if the system under consideration consists of independent particles, spatial correlations of ω_i vanish and the relation between the polarization and the response functions become trivial. In this case we simply have $C(\omega_i) = C^0(\omega_i) = 1$ and only the corresponding prefactors j_{ij}^0 and j_{ij}^0 occur in the expressions for the polarization.

E. Polarization

In addition to the approximations discussed above we assume that the parameters of the BO-model, ω_i and ω_i , are distributed according to some distribution functions $g(\omega_i)$ and $p(\omega_i)$, which we choose to be independent. For the density of states (DOS) of the low-frequency vibrations we will use $g(\omega_i) \propto \omega_i^m$, $m = 2; 4$ as they follow for the Debye model and the soft potential model, respectively. For computational convenience we additionally introduce a high-frequency cut-off ω_c :

$$g(\omega_i) = \frac{m+1}{\omega_c^{m+1}} \omega_i^m \quad (\omega_c > \omega_i) \quad (18)$$

With these approximations and definitions we have from eq.(6):

$$P^{(\alpha)}(t) \neq \frac{1}{m} E_M j_{ij}^0 j_{ij}^0 \sum_i \omega_i \sum_i g(\omega_i) p(\omega_i) C(\omega_i) R_i^{(\alpha)}(t) \quad (19)$$

and an analogous expression for the modulation, eq.(9):

$$P^{(\alpha)}(t; t_w; t_p) \neq \frac{3}{2m^3} E_M E_P^2 j_{ij}^0 j_{ij}^0 \sum_i \omega_i \sum_i g(\omega_i) p(\omega_i) 3C(\omega_i)^2 R_i^{(\alpha)}(t; t_w; t_p) \quad (20)$$

As already noted in connection with eq.(9) and in the previous section, the expression for $P_{(\text{harm})}^{(\kappa)}$ is obtained from the one for $P^{(\kappa)}$ by replacing $[\frac{\omega}{2} - \omega_i]^{0.4} C(\omega_i)^2$ by $[\frac{\omega}{2} - \omega_i]^{0.2} C(\omega_i) C^0(\omega_i)$ and using $R_{i;(\text{harm})}^{(\kappa)}$ instead of $R_i^{(\kappa)}$. These expressions will be used to discuss the response of a collection of Brownian oscillators to the NHB pulse sequence.

At this point it should be pointed out that in case of $\gamma > 0$ the sign of the two functions $P^{(\kappa)}$ and $P_{(\text{harm})}^{(\kappa)}$ will be the opposite. This is an example of the fact that one cannot predict the sign of a third-order response in general.

III. Results and Discussion

In this section we will discuss the results of model calculations and show that indeed the NHB field sequence is capable to detect dynamic heterogeneities provided they exist. In the discussion of the nonlinear modification we will mainly focus on $P^{(\kappa)}$ but also show results for $P_{(\text{harm})}^{(\kappa)}$. In addition we will give an order of magnitude estimate of the expected effects, as this is of utmost importance for possible experimental realizations.

A. Dielectric loss

We start with a brief discussion of the dielectric loss, $\omega(\omega)$. From eq.(19) and the Fourier transform of eq.(7) one obtains $\omega(\omega) = (\epsilon_0 E_M)^{-1} F[P^{(p)}(t)]$, where ϵ_0 is the permittivity of free space. For simplicity we restrict ourselves to a single damping constant, i.e. we use $p(\omega_i) = (\gamma_i)$ in eq.(19). We then explicitly have:

$$\omega(\omega) = \frac{1}{\epsilon_0 m} \sum_i \gamma_i^2 d\omega_i g(\omega_i) C(\omega_i) \frac{1}{(\omega_i^2 - \omega^2)^2 + (\gamma_i)^2} \quad (21)$$

The limiting behavior of $\omega(\omega)$ can easily be extracted from this expression. For vanishing γ eq.(21) reduces to $\omega(\omega) = (\epsilon_0 m)^{-1} (\gamma = 2) \sum_i \gamma_i^2 C(\omega_i) g(\omega_i) = \omega$ which is directly proportional to the Raman intensity scaled to the Bose factor. Using eq.(17) for $C(\omega_i)$ and eq.(18) for $g(\omega_i)$ this implies $\omega(\omega) \propto \omega^{m+n-1}$. For finite γ we have $\gamma > 0$ at low frequencies and therefore $\omega(\omega) \propto \omega$. For frequencies $\omega > \omega_c$ this behavior changes into that of undamped oscillations. Since the DOS has a high frequency cut-off ω_c we find for $\omega > \omega_c$ $\omega(\omega) \propto \omega^{-1}$ in the overdamped case and $\omega(\omega) \propto \omega^{-3}$ otherwise. This behavior is exemplified in Fig.2, where we plotted $\omega(\omega)$ versus ω/ω_c for $m = 2, n = 1$ and various values of the damping constant γ . Also included in Fig.2 as the thin dotted line is the dielectric loss for a Debye relaxation, $\omega_D(\omega) = \gamma/(\omega^2 + \gamma^2)$, which behaves as $\omega_D(\omega) \propto \omega^{-1}$ and $\omega_D(\omega) \propto \omega^{-3}$ for small and large ω , respectively. This shows that in the overdamped case we have an apparent distribution of relaxation times, giving rise to a sublinear increase of $\omega(\omega)$ for small ω . Of course, the cusp in $\omega(\omega)$ for small ω has its origin solely in the assumed high-frequency cut-off of $g(\omega)$.

B. Nonlinear modifications

Before we discuss the behavior of the modification $P^{(p)}(\omega; \tau_w; \tau_p)$ it is instructive to consider the response associated with a single mode q_i . In Fig.3 we show the real and imaginary parts of $R_i^{(p)}(\omega; \tau_w; \tau_p)$, the Fourier transform of $R_i^{(p)}(t; \tau_w; \tau_p)$ given in eq.(10), for a burn frequency $\omega = 1.0$. The full lines correspond to an underdamped oscillator whereas the dashed line represents the overdamped case. Note that $\hat{\omega}_i(\omega)$ in this situation only determines the overall amplitude of the modification. Only when a distribution of modes is considered the frequency selectivity of $\hat{\omega}_i(\omega)$ becomes important. In the present situation of a single mode this only means that the overall amplitude of $R_i^{(p)}(t; \tau_w; \tau_p)$ is changed if the burn frequency is varied. In the underdamped case a clear resonance occurring at $\omega = \omega_i$ is visible in both, $R_i^{(p)}(\omega; \tau_w; \tau_p)^{(0)}$ and $R_i^{(p)}(\omega; \tau_w; \tau_p)^{(1)}$. Additionally, a weak resonant behavior is found at $\omega = 3\omega_i$. This can be understood from the definition of h^p and g^p , cf. eq.(A.1), and stems from terms of the form $1 = [\beta_i - i!]$. On the other hand, in the overdamped case the maximum modification is found at $\omega = \omega_i$ (more precisely $\omega = 0.86 \omega_i$). In the limit of the OU-process, the result for $R_i^{(p)}$ has been given above in eq.(13). The factor ω_i^6 in the denominator explains the smallness of $R_i^{(p)}(\omega; \tau_w; \tau_p)^{(0,1)}$, which in Fig.3 was multiplied by a factor 10^8 . In this case of overdamped dynamics the imaginary part appears to be better suited to find the maximum modification. Thus, in the following we concentrate on $R_i^{(p)}(\omega; \tau_w; \tau_p)^{(0)}$ although in some situations the real part may also yield helpful information.

The behavior of $R_i^{(p)}(\omega; \tau_w; \tau_p)$ as a function of ω also determines the modification of the polarization, $P^{(p)}(\omega; \tau_w; \tau_p)$ according to eq.(20). In the upper panel of Fig.4a we plotted $P^{(p)}(\omega)^{(0)} = P^{(p)}(\omega; \tau_w; \tau_p)^{(0)}$ versus frequency for various pump-frequencies and one cycle of the pump-field. As in Fig.2, we chose $m = 2$ and $n = 1$, i.e. $g(\omega_i)/\omega_i^2, C(\omega_i) = \omega_i$. Additionally, we consider a single damping constant, thus writing $p(\omega_i) = (\omega_i - \gamma)$ with $\gamma = 10^{-2} \omega_i$ in eq.(20). We find that for all ω_i the minimum of the modification is observed at frequencies ω_{min} . In the lower panel $P^{(p)}_{(harm)}(\omega)^{(0)}$ is shown. In this calculation we assumed $C^0(\omega_i) = C(\omega_i)$ for simplicity and used the same parameters as in the upper panel. It is evident that the main differences are the reversed sign of the modification and that ω_{max} is slightly larger for all pump frequencies. Additionally, in the underdamped regime a slight minimum is observable at $\omega = \omega_i$, which is absent in $P^{(p)}(\omega)^{(0)}$. However, the most important conclusion that can be drawn from Fig.4a is that the modification of the response clearly exhibits a pronounced ω -selectivity. This means, that NHB is capable to 'detect' dynamic heterogeneities also in the regime of oscillatory motions.

In addition to the ω -selectivity we can discriminate between underdamped and overdamped modes due to the functional form of $P^{(p)}(\omega)^{(0)}$. In the overdamped regime the modification only shows a minimum, cf. eq.(13) (a maximum in case of $P^{(p)}_{(harm)}(\omega)^{(0)}$). In the underdamped case an additional dispersive behavior is observed. This means that also in the macroscopic polarization the main features already observed for the response of a

single mode persist. In Fig.4a, the dashed lines correspond to overdamped modes because here γ_i and thus mainly the response of those modes with γ_i is modified by the pump. For higher burn frequencies, however, mainly the response of underdamped modes is modified, cf. the full lines in Fig.4a. Here, the maximum modification is around $|\dot{\gamma}_i|$ and therefore $|\dot{\gamma}_i|' \approx 0$. Of course, for other choices of the damping constant the cross-over from underdamped to overdamped modes takes place at a different frequency.

If we compare the form of the modifications in the underdamped regime, the full lines in the upper panel of Fig.4a, to those for a single underdamped mode shown in Fig.3, it is evident immediately that the range of non-vanishing modification extends over a considerably larger $|\dot{\gamma}_i|$ -range. This has its origin mainly in the functional form of $\hat{\gamma}_i(\omega)$, cf. eq.(11), in particular the factor $(1 - e^{-i\omega t_p})$, which shows oscillatory behavior in the underdamped case. At low frequencies some more strongly damped modes contribute to the signal, rendering the modification broader as compared to Fig.3. This effect can be suppressed by increasing the number of cycles N of the sinusoidal pump-pulse. The condition $e^{-i\omega t_p} \approx 1$ is fulfilled for $N = (\gamma_i)$ and thus for a large number of cycles the behavior of a single oscillator is approached. Therefore, in the regime of underdamped modes the number of cycles N may turn out to be a useful experimental parameter. This is in contrast to the situation of overdamped modes where increasing N mainly gives rise to a small increase in the overall amplitude due to the factor $(1 - e^{-i\omega t_p})$.

Next, we consider the frequency at the minimum modification, $|\dot{\gamma}_{min}|$. This quantity is plotted versus ω in Fig.4b for two pairs of $(m;n)$. Remember that these parameters determine the effective distribution of $|\dot{\gamma}_i|$ contributing to the signal because according to eq.(20) we have $g(|\dot{\gamma}_i|)C(|\dot{\gamma}_i|)^2 / |\dot{\gamma}_i|^{m+2n}$. Due to this behavior, the equivalences $(2;1) \doteq (4;0)$ and $(2;2) \doteq (4;1)$ hold for the pairs $(m;n)$ shown. As in Fig.4a, the upper panel shows $|\dot{\gamma}_{min}|$ extracted from $P^{(P)}(|\dot{\gamma}|)^0$ and in the lower panel $|\dot{\gamma}_{max}|$ obtained from $P_{(harm)}^{(P)}(|\dot{\gamma}|)^0$ is plotted. In the latter case, we again assumed $C^0(|\dot{\gamma}_i|) = C(|\dot{\gamma}_i|)$. It is evident from Fig.4b that $|\dot{\gamma}_{min}| \neq 0$. Only in the regime of overdamped motion different pairs $(m;n)$ give rise to some minor differences in the values of $|\dot{\gamma}_{min}|$ ($|\dot{\gamma}_{max}|$). Of course, the linear relation $|\dot{\gamma}_{min}| / \omega$ has its origin in the form of the effective distribution of $|\dot{\gamma}_i|$ in the oscillatory regime and the corresponding distribution of $\gamma_i = |\dot{\gamma}_i|^2$ in the overdamped regime. In the underdamped case, one does not only have a minimum in $P^{(P)}(|\dot{\gamma}|)^0$ but also a maximum in addition, cf. Fig.4a. However, as discussed above, with increasing number of cycles, the differences between the minimum- and maximum-positions diminishes.

Sofar, we have considered the case of a fixed damping constant, which of course should be interpreted as an average value. It is evident from the discussion of Fig.4 that the value of γ can hardly be extracted from $P^{(P)}(|\dot{\gamma}; t_w; t_p)^0$ and this does not change if a distribution of damping constants is assumed in the calculations. On the other hand, it is known from previous studies that $P^{(S)}(t; t_w; t_p)$ is sensitive to relaxation rates and we thus expect the same for $P^{(P)}(t; t_w; t_p)$. In order to demonstrate that in the oscillatory regime measuring $P^{(P)}(t; t_w; t_p)$ may provide information about the damping constants,

in the upper panel of Fig.5 we plot this quantity versus measuring time for the same parameters as used in Fig.4. Here, we used $\beta_c = 0.1$ and various numbers of cycles of the pump field, N . The first thing to notice is that for $N = 1$ hardly any oscillations are visible in the time-domain, whereas this behavior changes with increasing N . This fact has the same origin as the decreasing broadening of the modulations for larger N , as discussed in context with Fig.4a. For a single cycle of the pump field $P^{(P)}(\omega; t_w; t_p)^{(0)}$ shows a very broad resonance and accordingly the dot-dashed line shows almost no oscillations. For $N = 10$ $P^{(P)}(\omega; t_w; t_p)$ shows the expected oscillatory behavior. More important for the present discussion, however, is the fact that for a large number of cycles it is evident that the signal has its maximum envelope around $\omega = \omega_1$. This is demonstrated by the dotted lines, which are of the form $\exp(-\gamma t)$. This functional form of the envelope can be derived analytically from the expression for the pulse-response of a single mode, eq.(10).

The lower panel of Fig.5 shows $P_{(narm)}^{(P)}(\omega; t_w; t_p)$ for the same parameters and the additional assumption $C^{(0)}(\omega_i) = C^{(1)}(\omega_i)$. In this case, however, the situation is quite different. Here the main effects are observed at $\omega = \omega_1$ and the oscillatory behavior around ω_1 is strongly suppressed. On the other hand, the maxima of the signal are by about a factor of ten smaller than in case of $P^{(P)}(\omega; t_w; t_p)$. (The envelope function (dotted line) is the same as in the upper panel but divided by a factor of 30.) Thus, we conclude that also in the oscillatory regime NHB experiments may be useful in order to get information about the damping, although this might require to perform experiments with various numbers of pump field cycles. In particular, this should be feasible if the main contribution to the signal stems from $P^{(P)}(\omega; t_w; t_p)$, i.e. for very small $j^{(0)}$.

C. Estimated magnitude of nonlinear effects

For an experimental realization of the NHB experiment in the THz regime it is of course desirable to have at least an order of magnitude estimate of the expected nonlinear effects. For this reason we consider the ratio $P = P_{NL}/P_{L}$, where P and P_{NL} are shorthand notations for the linear response and the nonlinear modulation. Experimentally, the sum $P_{tot} = P + P_{NL}$ will be observed and P_{NL} has to be extracted by a proper phase cycling procedure, cf. ref.[4].

We start our consideration with $P^{(1)}(\omega)^{(0)}$ for a single overdamped mode, given in eq.(13). For our rough estimate we consider the frequency of the maximum modulation, i.e. $\omega = \omega_1$, which allows us to neglect $\omega_i^{(0)}(\omega_i = 3)$ as compared to $\omega_i^{(0)}(\omega_i)$ and to use $\exp(-\gamma_i t_p) \approx 0$. Furthermore we set the waiting time to zero. This way we find:

$$\frac{P_{NL}}{P_L} \approx \frac{3 E_p^2 j_{ij}^{(0)2}}{8 m^2 \omega_i^4} \quad (4)$$

In order to proceed we replace the derivative of the dipole moment by $\dot{p}_i^{(0)}(\omega = \omega_1)$ and assume that $(\dot{p}_i^{(0)})^2$ is either related to the thermal expectation value $\langle \dot{p}_i^2 \rangle = (k_B T) = (m \omega_i^2)$

or the average displacement q_4^2 . This allows us to write

$$\frac{P}{P} = \frac{3}{8} \frac{E_p^2}{k_B T} q_4^2 \quad (22)$$

In order to proceed, we need an estimate of the quartic anharmonicity q_4 . For this purpose we utilize the detailed comparison of the predictions of the soft-potential model (where a potential of a similar form as in eq.(4) is used) with experimental results on a variety of different glassforming liquids[30]. From this comparison we find an average value of $q_4 \approx 2 \times 10^{-2}$. Assuming a value of j_1^0 on the order of $1 \text{ Db}/1\text{A}$ [31], the value of the actual displacement and the one to be chosen for q_4 are not independent of each other. If $q_4 = x \cdot 1\text{A}$ we should use $x \cdot 1 \text{ Db}$. Note that this gives an estimate for $q_4^2 \approx 2x^2 \times 10^{-4}$ which should be smaller than unity in order for the perturbation expansion used in Sect.II to be meaningful. Assuming a pump-field amplitude $E_p = z \cdot 10^4 \text{ kV/cm}$ one then finds, using $(10^4 \text{ kV/cm} \cdot 1 \text{ Db}) / (k_B \cdot 100 \text{ K}) \approx 2.5$, that $P/P = 5 \cdot 10^{-4} z^2$. Thus, for a reasonable value of $x \approx 0.05$ one has $P/P \approx 3 \cdot 10^{-3} z^2$, meaning that P/P is in the percent range for $z \approx 2$ or $E_p \approx 2 \cdot 10^4 \text{ kV/cm}$.

In this context, it should be mentioned, that the above estimate of course should not be used if one is concerned with the primary relaxation of high temperature liquids. This is because in that case the dielectric relaxation is mainly determined by the mean square fluctuations, $\langle h^2 \rangle$, of the static molecular dipole moment due to the molecular tumbling motion. In our formulation this means that we loosely should identify $\langle q^2 \rangle \approx q_4^2$ with $\langle h^2 \rangle$, cf. ref.[12]. Assuming isotropic rotational jumps as a simple but realistic model for the stochastic reorientational motion in liquids[32] allows us to identify q_4 with a 'rotational jump length', $q_4 \approx R_H \sin(\theta_{\text{rot}})$. Here, the hydrodynamic radius R_H is on the order of 1A [33], yielding $q_4^2 \approx 6$, if the mean jump angle θ_{rot} is on the order of ten degrees. Again we write $E_p = z \cdot 10^4 \text{ kV/cm}$ in eq.(22), but now we use $T = 300 \text{ K}$. For a dipole moment of 1 Db this gives $(P/P)_{(\text{rot}; 300 \text{ K})} \approx 4z^2$. Therefore, a pump-field amplitude of $E_p \approx 500 \text{ kV/cm}$ is sufficient to get an effect in the percent range. This value is in harmony with the amplitudes used in the NHB experiments on supercooled liquids[4].

Next, we consider the more relevant case of underdamped oscillatory motion. In order to give an estimate of the ratio $P(\omega)/P(\omega)^0$ in this regime we now consider a distribution of eigenfrequencies ω_i similar to the discussion in context with Fig. 4a (upper panel) and $C(\omega_i)/\omega_i$. The expression for the dielectric loss, eq.(21), allows us to write

$$\frac{P(\omega)^0}{P(\omega)^0} = \frac{9}{2} \omega^0(\omega)^{-1} E_p^2 \frac{\sum_i^R d\omega_i g(\omega_i) \omega_i^2 R_i^{(P)}(\omega)^0}{\sum_i^R d\omega_i g(\omega_i) \omega_i R_i^{(P)}(\omega)^0} \quad (23)$$

In this expression, $\rho_m = m \approx 10^3 \text{ kg/m}^3$ is the samples mass density. In order to obtain a peak in the THz-range we now use a DOS of the form $g(\omega_i)/\omega_i^2 \exp(-\gamma/\omega_i)$, with $\gamma = 4 \cdot 3 \cdot 10^{12} \text{ Hz}^{-1}$, yielding a peak at $\omega_i = 1.5 \text{ THz}$. Consequently, we set $\gamma = 1.5 \text{ THz}$. Additionally,

we fix the damping constant to value of $\gamma = 0.1 \text{ THz}$. We point out, that a variation of γ has only a minor effect on the resulting amplitudes as long as the motion is in the strongly underdamped regime. For the dielectric loss in the THz-range we approximately have $\epsilon''(\text{THz}) \approx 1$, as found for glycerol[34]. Evaluating the integrals in eq.(23) at $\omega_{\text{in}} \approx 1 \text{ THz}$ (cf. Fig.4) allows us to calculate P_{max} . For γ we use the same value as before, $\gamma \approx 10^{22} \text{ m}^{-2}$ and find

$$\frac{P_{\text{max}}}{P}(\text{THz}) \approx 3 \cdot 10^5 \frac{E_p^2}{(V_{\text{cm}})^2}$$

This way we obtain $P_{\text{max}} = P \approx 0.3$ for a pump-field amplitude of $E_p = 10^2 \text{ kV/cm}$. These considerations allow us to conclude that – with the assumptions used – the ratio $P = P_{\text{nonlinear}}/P_{\text{linear}}$ should be larger in the oscillatory regime than in the overdamped regime. Of course, from an intuitive point of view this does not come as a surprise because some resonant behavior even is expected in this case.

Sofar, we have considered the nonlinear modification $P(\omega)$. We close this section with a brief discussion of the relative magnitudes of P and $P_{\text{(harm.)}}$, the nonlinear modification stemming from the second order term in the expansion of the dipole moment, eq.(3). As is evident from Fig.4a, the magnitudes of the normalized effects are quite similar. Thus, we have to compare the prefactors $3 \cdot \gamma \omega_j^0$ and $\gamma \omega_j^0$. For this purpose we proceed in exactly the same way as we did in the discussion of the overdamped motion. We approximate $\gamma \omega_j^0$ by $(\gamma \omega_j^0) = \hbar q^2 i$ and $\gamma \omega_j^0$ by $(\gamma \omega_j^0) = (3 \hbar q^2 i q^2)$. This way we find for the ratio

$$\frac{3 \cdot \gamma \omega_j^0}{\gamma \omega_j^0} \approx 9 q^2 \approx \frac{1}{[\dots]} \approx 2 \times 10^{-2} \frac{1}{[\dots]}$$

If we now assume that $\omega_j^0 \approx 1 \text{ Db}$ and simply by analogy that $[\dots]^2 \approx 1 \text{ Db}$, we have $3 \cdot \gamma \omega_j^0 \approx 2 \cdot 10^{-2} \gamma \omega_j^0$ and thus a negligible effect due to $P_{\text{(harm.)}}$. However, it should be borne in mind that apart from the necessity of estimating $[\dots]$ also the function $C(\omega_j)$ occurring in the expression for $P_{\text{(harm.)}}$ is unknown. On the other hand, an experimental determination of the relative relevance of P and $P_{\text{(harm.)}}$ appears feasible due to the fact that the effects are of opposite sign.

IV. Conclusions

We have calculated the response of a system consisting of a collection of Brownian oscillators to the NHB field sequence. For simplicity, we have restricted ourselves to a classical calculation and assumed Ohmic friction, i.e. time-independent damping constants. A more general case will be treated in a separate publication [20]. Furthermore, we have restricted the calculations to a quadratic expansion of the dipole moment in the normal mode coordinates q_i and included no higher terms than the quartic anharmonicity ($\propto q_i^4$) in the potential. We did not allow for any coupling among the modes. We do not expect that

any of these assumptions presents a severe restriction on the applicability of our results. Additionally, we expect a similar behavior in case that the light couples predominantly to the polarizability instead of the dipole moment.

We have applied our calculation to the situation encountered in amorphous systems in the frequency range of the so-called boson peak. We do not claim that a BO-model quantitatively describes the features of the vibrational excitations in this frequency regime. However, there appears to be some consensus about the quasi-harmonic nature of these vibrations. Although different models for the dynamics in the boson peak regime attribute different damping mechanisms [26, 35, 36], experimental results often can be fitted to a simple damped oscillator susceptibility function [37]. Because less is known about the detailed form of the DOS in the THz range, we simply parameterized it as $g(\omega) \propto \omega^{-m}$. In contrast to the situation of low-frequency Raman scattering, we are concerned with a nonlinear response and therefore have to face four-point spatial correlation functions of some elasto-optical constants. In a simple mean-field treatment we factorized these four-point correlation functions. For the various contributions to the nonlinear response different two-point correlation functions are relevant. We have focussed predominantly on the contribution that depends on the square of the so-called light to vibration coupling. For the latter, we used a functional form $C(\omega) \propto \omega^{-n}$ with various values for n in order to be as flexible as possible and not to rely on some specific model. Along with the behavior of the DOS we thus can investigate the behavior for models ranging from Debye-like phonons [24] to soft-potential quasi-harmonic modes [26].

Our main finding is that also in the regime of oscillatory motions is NHB able to 'detect' dynamic heterogeneities via a pump-frequency selective modification of the linear response. In contrast to slow relaxation processes, where usually the response to a step field is monitored in the time domain it seems to be advantageous to consider the Fourier-transform of the response to a field pulse in case of underdamped motion. For all relevant pairs (m, n) we find a linear relation between the frequency of the maximum modification and the pump-frequency. For underdamped modes oscillators with $\omega_i \ll \omega_p$ are addressed primarily whereas in the overdamped case those with $\omega_i \approx \omega_p$ are most relevant. The latter situation is similar to what has been found in earlier investigations. If the dynamic range of the experiment is large enough, a cross-over from underdamped oscillations to overdamped relaxation should be observable in principle.

An important point in the context of nonlinear response functions regards the relation between the pulse- and the step-response. Whereas these functions are trivially related in the linear regime this has been shown not to be the case for the nonlinear modifications. We explicitly demonstrated this behavior for the strongly overdamped case, i.e. the OU limit. For this case a modification of the step-response has been found which is very similar to the expression given earlier for a model of stochastic dipole reorientations [12].

Regarding the magnitude of the expected nonlinear effects, we estimate that pump-field amplitudes on the order of 10^2 – 10^3 kV/cm should suffice to find nonlinear modifications

which are on the order of one percent of the linear response of the system. With the newest technical achievements, this leads us to conclude that the experimental realization of NHB and other nonlinear experiments in the THz regime should be practicable.

In conclusion, we have shown that NHB experiments in the THz region are expected to yield valuable information about the physical origin of the long-discussed vibrations around the boson peak. In particular the question as to which extent the dynamics in this regime has to be viewed as dynamic heterogeneous can be answered, thus shedding further light on the nature of the dynamics in disordered systems.

Acknowledgements:

We are grateful to R. Schilling and K. A. Nelson for fruitful discussions on the topic and the reading of a first version of the manuscript. This work was supported by the DFG under Contract No. D i693/1-1.

Appendix

In this Appendix we give the explicit expressions for the modification of the response, $R_i^{(x)}(t; t_w; t_p)$, that are used in the text.

Using the abbreviation

$$h_{a;b}(t) = h_{b;a}(t) = \frac{1}{a-b} e^{at} - e^{bt}$$

the functions $h^x(a; b; t)$ and $g^x(a; b; t)$ are given by:

$$\begin{aligned} h^P(a; b; t) &= \frac{1}{b} [h_{3b;a}(t) - h_{a+2b;b}(t)] \\ g^P(a; b; t) &= \frac{2}{a+b} [h_{a+2b;a}(t) - h_{b+2a;b}(t)] \end{aligned} \quad (A.1)$$

$$\begin{aligned} h^S(a; b; t) &= \frac{1}{b^2} [h_{2b;a}(t) + h_{a+2b;2b}(t) - h_{3b;a}(t) - h_{a+2b;b}(t)] \\ g^S(a; b; t) &= \frac{2}{a+b} h_{a+b=2, b=2}^2(t) - h_{b+a=2, a=2}^2(t) \end{aligned} \quad (A.2)$$

and

$$\begin{aligned} h^{AC}(a; b; t) &= \frac{1}{b} \frac{1}{a+b} (h_{2b+i!, 2b+a}(t) - h_{2b+i!, b}(t)) \\ &\quad + \frac{1}{3b} \frac{1}{a} (h_{2b+i!, a}(t) - h_{2b+i!, 3b}(t)) \\ g^{AC}(a; b; t) &= \frac{2}{a+b} \frac{1}{a} (h_{a+b+i!, 2a+b}(t) - h_{a+b+i!, b}(t)) \\ &\quad - \frac{1}{b} (h_{a+b+i!, 2b+a}(t) - h_{a+b+i!, a}(t)) \end{aligned} \quad (A.3)$$

In order to calculate the Fourier transform of $R_i^{(P)}(t)$ and $R_i^{(P)}(t; t_w; t_p)$ it is sufficient to note that these can easily be obtained from eqns.(7) and (10) by noting that

$$F[h_{a;b}(t)] = \frac{1}{a-b} \frac{1}{a-i!} - \frac{1}{b-i!} :$$

References

- [1] for reviews see: H. Sillescu; J. Non-Cryst. Solids 243 81 (1999); R. Bohmer; Curr. Opinion in Solid State and Mater. Sci. 3 378 (1998); M. D. Ediger, C. A. Angell and S. R. Nagel; J. Phys. Chem. 100 13200 (1996);
- [2] K. Schmidt-Rohr and H. W. Spiess; Phys. Rev. Lett. 66 3020 (1991)
- [3] M. T. Cicerone and M. D. Ediger; J. Chem. Phys. 103 5684 (1995)
- [4] B. Schiener, R. Bohmer, A. Loidl and R. V. Chamberlin; Science 274 752 (1996); B. Schiener, R. V. Chamberlin, G. Diezmann and R. Bohmer; J. Chem. Phys. 107 7746 (1997)
- [5] A. Heuer, M. Wilhelm, H. Zimmermann and H. W. Spiess; Phys. Rev. Lett. 75 2851 (1995); R. Bohmer, G. Hinze, G. Diezmann, B. Geil and H. Sillescu; Europhys. Lett. 36 55 (1996)
- [6] R. Bohmer, R. V. Chamberlin, G. Diezmann, B. Geil, A. Heuer, G. Hinze, S. C. Kuebler, R. Richert, B. Schiener, H. Sillescu, H. W. Spiess, U. Tracht and M. Wilhelm; J. Non-Cryst. Solids 235-237 1 (1998)
- [7] R. Kubo, M. Toda and N. Hashitsume: Statistical Physics II Springer, Berlin-Heidelberg-New York (1992)
- [8] K. Duivvuri and R. Richert; J. Chem. Phys. 118 1356 (2003)
- [9] O. Kircher, B. Schiener and R. Bohmer; Phys. Rev. Lett. 81 4520 (1998)
- [10] R. Richert and R. Bohmer; Phys. Rev. Lett. 83 4337 (1999)
- [11] R. V. Chamberlin; Phys. Rev. Lett. 83 5134 (1999)
- [12] G. Diezmann; Europhys. Lett. 53 604 (2001)
- [13] R. Bohmer and G. Diezmann; in Broadband Dielectric Spectroscopy, Eds. F. Kremer and A. Schonhals, Springer, Berlin (2002)
- [14] S. Mukamel: Principles of Nonlinear Optical Spectroscopy, Oxford, New York, Oxford (1995)
- [15] P. Schellenberg and J. Friedrich; in Disorder Effects on Relaxational Processes, Eds. R. Richert and A. Blumen, Springer, Berlin (1994)
- [16] A. P. Sokolov, E. Rossler, A. Kisliuk and D. Quitmann; Phys. Rev. Lett. 71 2062 (1993)

- [17] W .C .Beard, G .M .Turner and C .A .Schmuttenmaer; J.Phys.Chem .B 100 7146 (2002)
- [18] X .C .Zhang, B .Hu, J.T .Darrow and D .H .Austin; Appl.Phys. 56 1011 (1990)
- [19] K .A .Nelson, private communication
- [20] U .Haberle and G .Diezemann; to be published
- [21] R .Shuker and R .W .Gammon; Phys.Rev.Lett. 25 222 (1970)
- [22] K .Okumura and Y .Tanimura; Chem .Phys.Lett. 295 298 (1998)
- [23] N .G .van Kampen: Stochastic Processes in Physics and Chemistry, North-Holland, Amsterdam , New York, Oxford (1981)
- [24] A .J.Martin and W .Brenig; phys.stat.sol. (b) 64 163 (1974)
- [25] N .Ahmad; Phys.Rev.B 48 13512 (1993)
- [26] Y .M .Galperin, V .G .Karpov and V .I .Kozub; Adv.Phys. 38 669 (1989)
- [27] V .K .Malinovsky, V .N .Novikov, P .P .Parshin, A .P .Sokolov and M .G .Zemlyanov; Europhys.Lett. 11 43 (1990)
- [28] A .Fontana, R .Dell'Anna, M .Montagne, F .Rossi, G .Viliani, G .Ruocco, M .Sam - polino, U .Buchenau and A .W ischnewski; Europhys.Lett. 47 56 (1999)
- [29] N .V .Surovtsev, J .W iedersich, V .N .Novikov, E .Rossler and E .Duval; Phys.Rev.Lett. 82 4476 (1999)
- [30] D .A .Parshin; Phys.Rev.B 49 9400 (1994)
- [31] D .C .Harris and M .D .Bertolucci: Symmetry and Spectroscopy, Dover, New York (1989)
- [32] G .Diezemann, R .Bohmer, G .Hinze and H .Sillescu; J.Non-Cryst.Solids 235-237 121 (1998)
- [33] I .Chang and H .Sillescu; J.Phys.Chem .B 101 8794 (1997)
- [34] P .Lunkenheimer, A .Pimenov, M .Dressel, Y .G .Goncharov, R .Bohmer and A .Loidl; Phys.Rev.Lett. 77 318 (1996)
- [35] W .Schimacher, G .Diezemann and C .Ganter; Phys.Rev.Lett. 81 136 (1998)
- [36] V .N .Novikov; J.Non-Cryst.Solids 235-237 196 (1998)

- [37] C. Masciovecchio, G. Monaco, G. Ruocco, F. Sette, A. Cunsolo, M. Krich, A. Mermet, M. Soltwisch and R. Verbeni; Phys. Rev. Lett. 80 544 (1998)

Figure captions

Fig.1 : The field sequence for the nonresonant hole burning (NHB) experiment: One or more cycles of a strong sinusoidal field $E_P(t) = E_P \sin(\omega_P t)$ are applied to a sample in thermal equilibrium. After a waiting time t_w the response to a small field $E_M(t)$ is monitored.

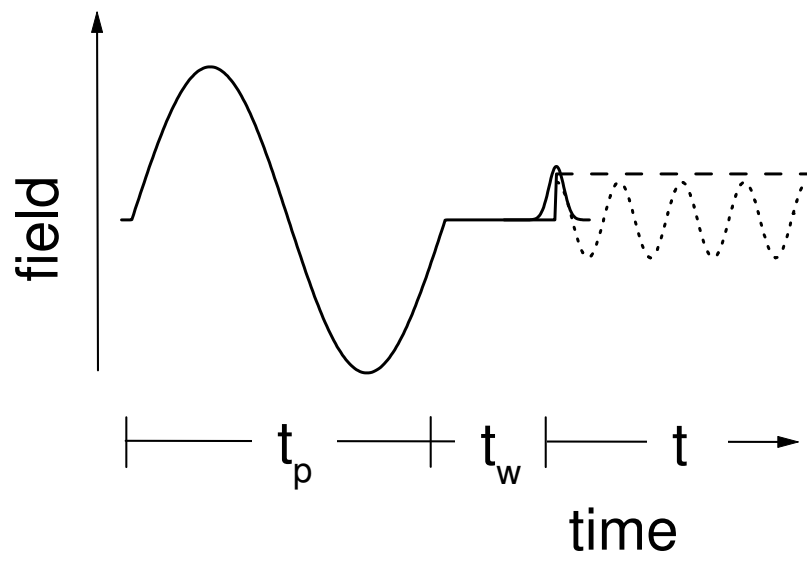
Fig.2 : The dielectric loss $\epsilon''(\omega)$ according to eq.(21) versus frequency for $g(\omega_i) = (3 - \omega_i^2) \omega_i^2 / (\omega_c^2 - \omega_i^2)$, $C(\omega_i) = \omega_i$ and $(m_0) j^0 j^2 = 1$. The damping constant is chosen as $\gamma = 0.01; 0.1; 1.0; 100$ and $\omega_c = 10$. from bottom to top. Also shown is $\epsilon_D''(\omega)$ for a Debye relaxation (thin dotted line) for comparison. Note that for $\gamma = 100$ the motion is strongly overdamped in the whole frequency range.

Fig.3 : Imaginary (upper panel) and real (lower panel) part of $R_i^{(P)}(\omega; t_w; t_p)$ (abbreviated as $R_i^{(P)}(\omega)$) versus measuring frequency ω for $\omega_i = 1.0$; $\gamma_i = 0.2$ (full lines; underdamped case) and $\omega_i = 10.0$; $\gamma_i = 100.0$ (dashed lines; overdamped case). One cycle of the sinusoidal pump field with frequency $\omega_P = 1.0$ has been used and the waiting was set to zero, $t_w = 0$. $R_i^{(P)}(\omega; t_w; t_p)$ is obtained from $R_i^{(P)}(t; t_w; t_p)$, eq.(10), via Fourier transform as explained in the text. The results for the overdamped case are multiplied by a factor 10^8 .

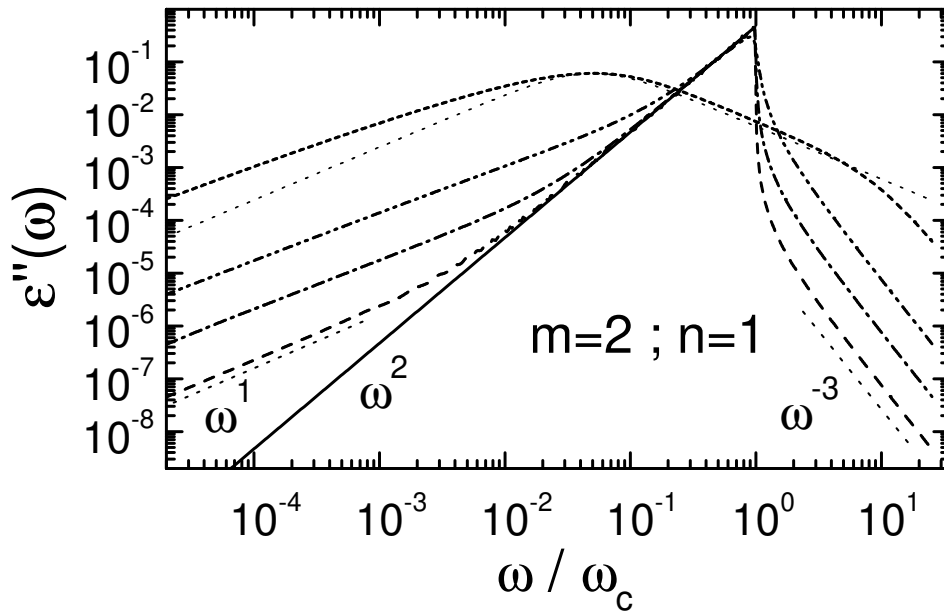
Fig.4 : a: $P^{(P)}(\omega)^\omega$ versus ω for various burn frequencies ω_P (upper panel). The DOS and the light to vibration coupling constant are the same as in Fig.2. The other parameters are $(3 - m^3 \omega_P^2 E_M^2 j^0 j^2) = 1$, $t_w = 0$ and $\gamma = 10^2 \omega_c$. The burn frequencies are chosen as $\omega_P = \omega_c = 0.0003; 0.001; 0.003$ (dashed lines) and $\omega_P = \omega_c = 0.01; 0.03; 0.1; 0.3$ (full lines). The dashed lines present overdamped oscillators while the full lines correspond to underdamped modes. In the lower panel $P_{(harm)}^{(P)}(\omega)^\omega$ is plotted, where additionally $C^0(\omega_i) = C(\omega_i)$ is assumed and we set $(-m^3 E_M E_P^2 j^0 j^2 j^0 j^2) = 1$.

b: Upper panel: The frequency at which $P^{(P)}(\omega)^\omega$ takes its minimum value (cf. Fig.4a), $\omega_{min} = \omega_c$ versus burn frequency ω_P . Lower panel: $\omega_{max} = \omega_c$ versus ω_P for $P_{(harm)}^{(P)}(\omega)^\omega$. The parameters for the DOS and the light to vibration coupling constants are written as $g(\omega) / \omega^m$ and $C(\omega) = \omega^n$. The results shown are for two pairs (m, n) and a damping constant $\gamma = 10^2 \omega_c$.

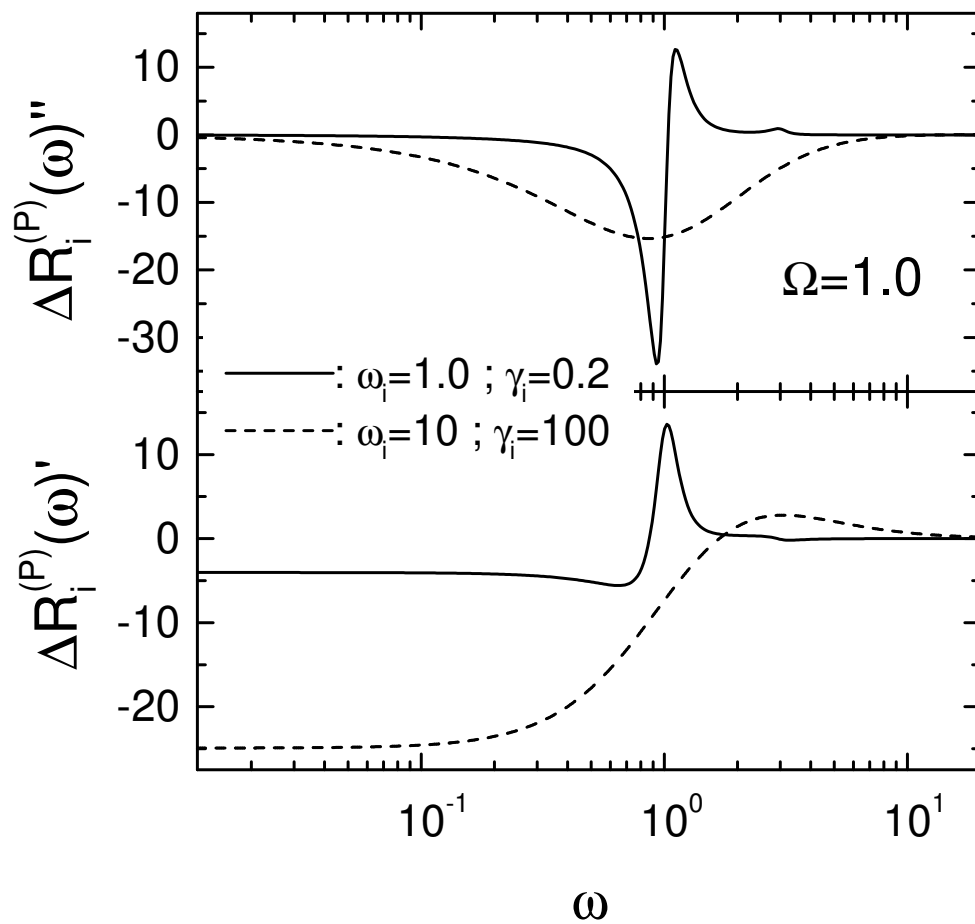
Fig.5 : $R_i^{(P)}(t; t_w; t_p)$ (upper panel) and $R_{(harm)}^{(P)}(t; t_w; t_p)$ (lower panel) versus measuring time for the same parameters as used in Fig.4, $\omega_P = 0.1$ and various numbers of pump field cycles, N . The dotted envelopes are of the form $t e^{-t}$. In the lower panel, the envelope has been divided by a factor of 30.



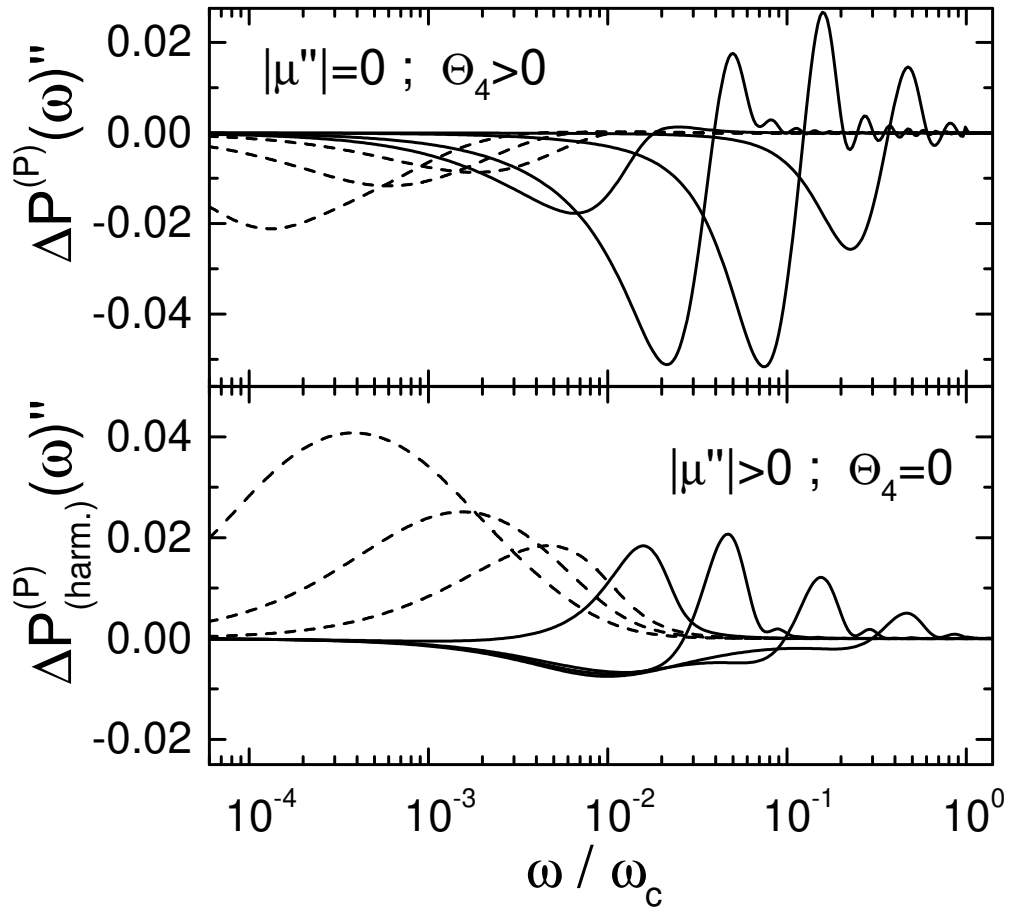
Häberle and Diezemann; Fig.1



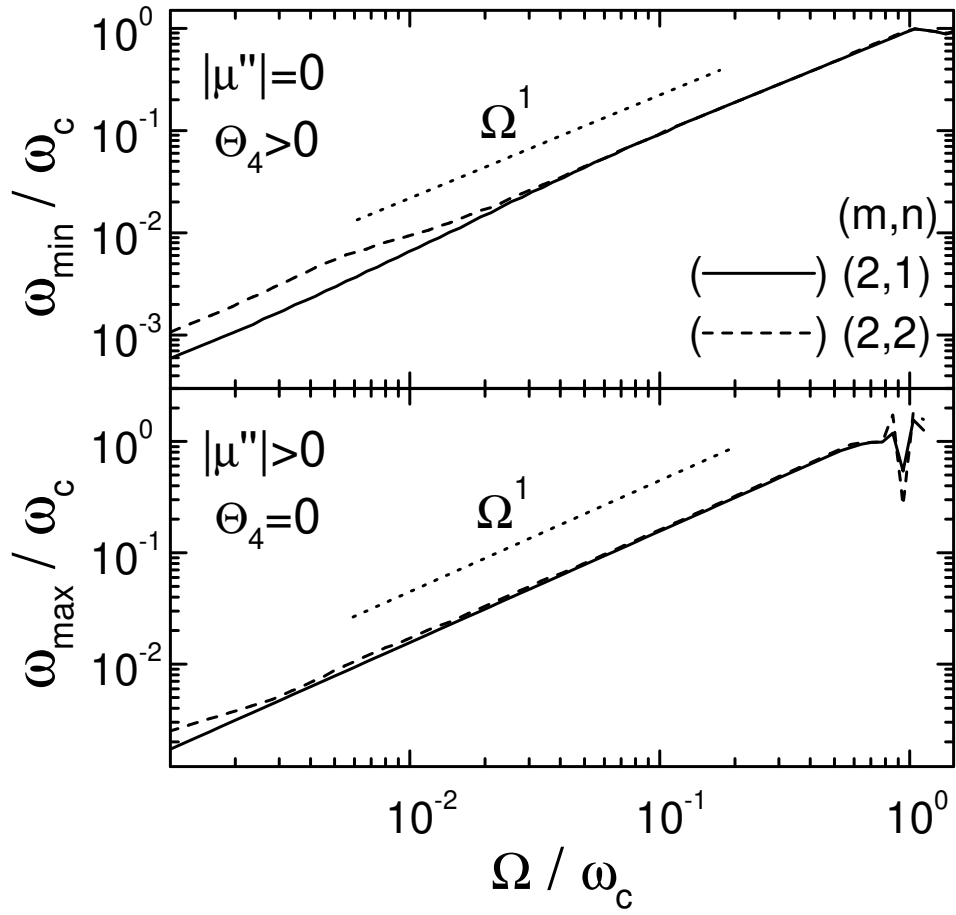
Häberle and Diezemann; Fig.2



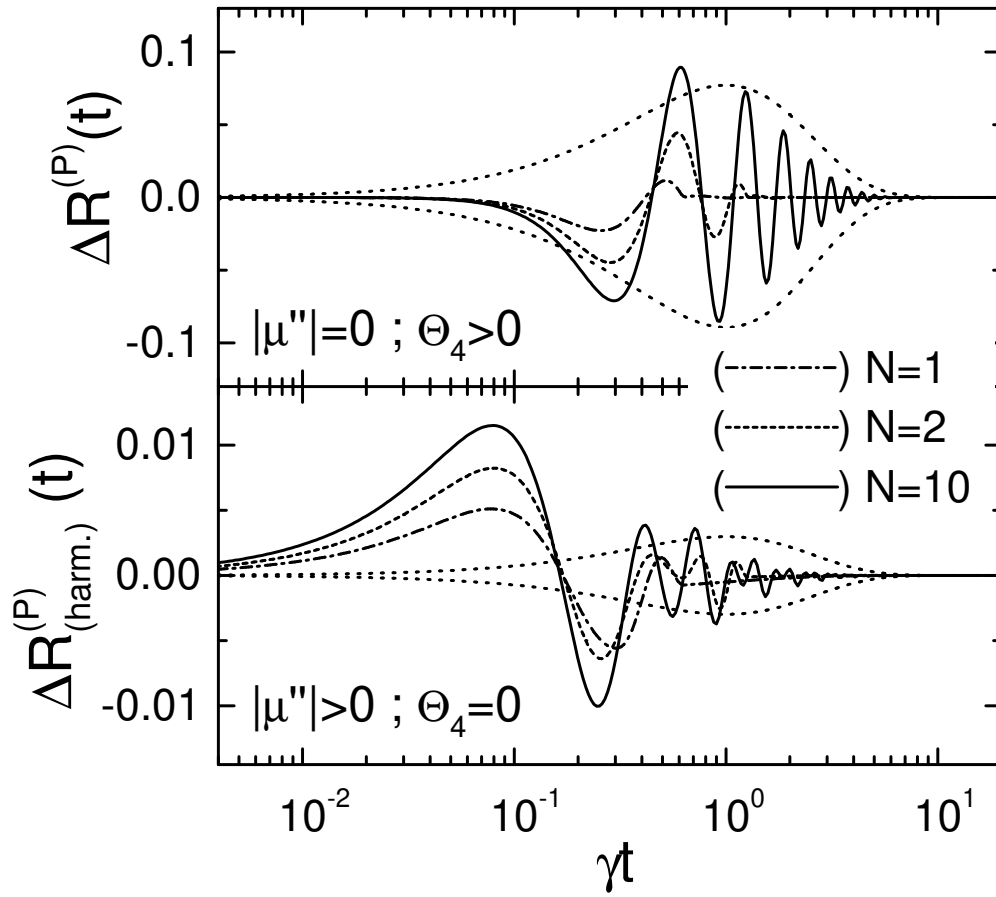
Häberle and Diezemann, Fig.3



Häberle and Diezemann, Fig.4a



Häberle and Diezemann, Fig.4b



Häberle and Diezemann, Fig.5